

Targeting malignant B cells with an immunotoxin against ROR1

Sivasubramanian Baskar,^{1,*} Adrian Wiestner,² Wyndham H. Wilson,³ Ira Pastan⁴ and Christoph Rader¹

¹Experimental Transplantation and Immunology Branch; Center for Cancer Research; National Cancer Institute; ²Hematology Branch; National Heart, Lung and Blood Institute;

³Metabolism Branch; Center for Cancer Research; National Cancer Institute; ⁴Laboratory of Molecular Biology; Center for Cancer Research; National Cancer Institute; National Institutes of Health; Bethesda, MD USA

Keywords: ROR1, immunotoxin, monoclonal antibody, chronic lymphocytic leukemia, mantle cell lymphoma

Abbreviations: CLL, chronic lymphocytic leukemia, MCL, mantle cell lymphoma, NHL, non-Hodgkin lymphoma; RTK, receptor tyrosine kinases; ROR1, receptor tyrosine kinase-like orphan receptor 1; hROR1, human ROR1; mROR1, mouse ROR1; mAbs, monoclonal antibodies; pAbs, polyclonal antibodies; STAT-3, signal transducer and activator of transcription 3; PBMC, peripheral blood mononuclear cells; FBS, fetal bovine serum; PBS, phosphate buffered saline; PAO, phenylarsine oxide; PS, phosphatidyl serine; BSA, bovine serum albumin; HRP, horseradish peroxidase; HRP conjugated-DaM, donkey anti-mouse; -DaR, donkey anti-rabbit; -DaG, donkey anti-goat; MFI, mean fluorescence intensity; FC, flow cell; RU, resonance units; ABB, annexin-V binding buffer; P.I., propidium iodide; CDC, complement dependent cytotoxicity; ADCC, antibody dependent cellular cytotoxicity; mIgG, normal mouse immunoglobulin; rIgG, normal rabbit immunoglobulin; Dy-GaM, DyLight-649 conjugated affinity pure F(ab)₂ preparation of goat anti-mouse IgG; Dy-GaR, DyLight-649 conjugated affinity pure F(ab)₂ preparation of goat anti-rabbit IgG; APC-GaM, allophycocyanin conjugated goat anti-mouse IgG Fc fragment specific; RaPEA, rabbit anti-pseudomonas exotoxin A; ELISA, enzyme-linked immunosorbent assay; SDS-PAGE, sodium dodecyl sulfate polyacrylamide gel electrophoresis; PE, phycoerythrin; SA-PE, streptavidin-conjugated PE

The selective cell surface expression of receptor tyrosine kinase-like orphan receptor 1 (ROR1) in chronic lymphocytic leukemia (CLL) and mantle cell lymphoma (MCL) has made ROR1 a novel and promising target for therapeutic monoclonal antibodies (mAbs). Four mouse mAbs generated by hybridoma technology exhibited specific binding to human ROR1 (hROR1). Epitope mapping studies showed that two mAbs (2A2 and 2D11) recognized N-terminal epitopes in the extracellular region of ROR1 and the other two (1A1 and 1A7) recognized C-terminal epitopes. A ROR1-immunotoxin (BT-1) consisting of truncated Pseudomonas exotoxin A (PE38) and the V_H and V_L fragments of 2A2-IgG was made recombinantly. Both 2A2-IgG and BT-1 showed dose-dependent and selective binding to primary CLL and MCL cells and MCL cell lines. Kinetic analyses revealed 0.12-nM (2A2-IgG) to 65-nM (BT-1) avidity/affinity to hROR1, depicting bivalent and monovalent interactions, respectively. After binding to cell surface ROR1, 2A2-IgG and BT-1 were partially internalized by primary CLL cells and MCL cell lines, and BT-1 induced profound apoptosis of ROR1-expressing MCL cell lines in vitro (EC₅₀ = 16 pM–16 nM), but did not affect ROR1-negative cell lines. Our data suggest that ROR1-immunotoxins such as BT-1 could serve as targeted therapeutic agents for ROR1-expressing B cell malignancies and other cancers.

Introduction

Receptor tyrosine kinases (RTKs) are known to be key regulators of normal cellular processes such as differentiation, migration, proliferation and survival, but they also have a critical role in the development and progression of many types of human cancers. Consequently, RTKs and their ligands have become attractive molecular targets for therapeutic interventions of cancer. The ROR family of RTKs consists of two evolutionarily conserved proteins, ROR1 and ROR2¹ and gene expression profiling identified ROR1 as one of the signature genes overexpressed in CLL.^{2,3} Subsequent reports showed a variety of cancer cell lines

and primary cancer cells of different histological origin expressed significant levels of ROR1 mRNA.^{4,5} Screening of the human kinome revealed ROR1 as one of the few potent survival kinases,⁶ and siRNA-mediated silencing of ROR1 induced apoptosis in CLL cells.⁷ ROR1 protein levels increased following IL-6-induced phosphorylation of a transcription factor, signal transducer and activator of transcription 3 (STAT-3), in myeloma cells, and overexpression of STAT-3, multiple Wnt genes and Wnt receptor Frizzled was observed in CLL cells.⁸ Unlike other RTKs, ROR1 is catalytically inactive and is transphosphorylated by the Met oncogene.⁵ Together, these findings suggest that ROR1 could provide survival signals and may contribute in the

*Correspondence to: Sivasubramanian Baskar; Email: baskars@mail.nih.gov

Submitted: 02/02/12; Revised: 02/29/12; Accepted: 03/01/12

<http://dx.doi.org/10.4161/mabs.19870>

development of leukemia. Studies from our laboratory and others have demonstrated the uniform and restricted cell surface expression of ROR1 protein in CLL.⁹⁻¹¹ We therefore hypothesized that ROR1 could serve as a target antigen for mAb based therapeutics.

B-cell malignancies are susceptible to therapeutic intervention by mAbs, and rituximab and ofatumumab, both of which target CD20 on all B cells (malignant and normal), and alemtuzumab, which targets CD52 on all leukocytes (malignant and normal), are FDA-approved for B-cell non-Hodgkin lymphoma (B-NHL) or CLL. Mechanistically, these three unarmed mAbs mediate direct cytotoxicity, complement dependent cytotoxicity (CDC) or antibody dependent cellular cytotoxicity (ADCC), and their efficacy depends on the availability of functional effector cells/molecules in the recipient. Although treatment with these mAbs has achieved significant progression-free survival and short-term overall survival benefits, most patients relapse or develop resistance. Therefore, there is a need for identification of new targets and development of novel therapeutics. In this context, mAbs against ROR1 would be welcome as they could specifically target malignant B cells, thereby sparing normal B cells and other leukocytes. Interestingly, patients with CLL produced endogenous anti-ROR1 antibodies following vaccination with CD40L-expressing autologous tumor cells,¹⁰ and following administration of the immunomodulatory drug lenalidomide,¹² which upregulated CD40L expression *in vitro*. These observations suggest that antibodies directed against ROR1 *per se* may not cause any adverse events *in vivo*, although their contribution to alleviate the disease remains to be understood. The restricted expression of cell surface ROR1 on malignant B cells and the apparent safety of an endogenous anti-ROR1 antibody response, prompted us to develop a ROR1-immunotoxin. Unlike unarmed mAbs, a ROR1-immunotoxin could specifically recognize and kill the target cells independent of effector components (complement proteins, NK cells, macrophages or T cells) that may not be optimally available in cancer patients. Immunotoxins are fusion proteins consisting of a target antigen-binding moiety (a ligand or mAb) that confers specificity, and a toxin moiety (from a plant or bacterium) that mediates target cell killing.^{13,14} Chemical conjugation of mAb and toxin has resulted in heterogeneous products unsuitable for clinical applications; this problem was overcome by genetic engineering wherein gene(s) encoding an antibody fragment are linked to a gene encoding selected toxin domains.¹⁴⁻¹⁸ A variety of immunotoxins with different antigen target specificities and different toxins have been developed to treat human cancers.¹⁹⁻²² We used truncated pseudomonas exotoxin A (PE38) because the functional domains of this toxin have been well characterized and the mechanisms of killing are known.^{16,23} Several PE38-based immunotoxins have been developed and are currently in clinical trials for different human disease indications, including B-cell malignancies.^{20,24-27} We describe here the generation and functional characterization of the PE38-based immunotoxin BT-1 directed against ROR1.

Results

Specificity and epitope mapping of anti-hROR1 mAbs and BT-1. The specificity of mAbs (2A2-IgG, 2D11-IgG 1A1-IgG

and 1A7-IgG), and the epitopes they recognized were determined by studying their reactivity against a panel of recombinant fusion proteins using ELISA (Fig. 1). All four mAbs exhibited strong binding to Fc-hROR1 and hROR1-ECD in a concentration-dependent manner (range tested 10 µg/mL to 1.5 ng/mL, data shown for only 1 µg/mL), but not to human Fc, hROR2-Fc or BSA indicating their specific reactivity to purified hROR1. In addition, while both 2A2-IgG and 2D11-IgG were able to bind Fc-hROR1Ig+Fz, only 2A2-IgG bound to Fc-hROR1Ig and neither mAb bound to Fc-hROR1Fz, Fc-hROR1Kr or Fc-hROR1Fz+Kr proteins. This pattern of reactivity suggested that the epitope recognized by mAb 2A2 is likely located in the Ig domain of hROR1 and that of 2D11 mAb is shared between Ig and Fz domains. Conversely, both 1A1-IgG and 1A7-IgG were able to bind Fc-hROR1Fz+Kr and Fc-hROR1Kr, but not to Fc-hROR1Ig+Fz, Fc-hROR1Ig or Fc-hROR1Fz proteins, suggesting that the epitopes recognized by these two mAbs are likely located in the Kr domain of hROR1. As positive controls, GaROR1 pAbs demonstrated specific binding to all recombinant hROR1 proteins and GaROR2 pAbs to the recombinant hROR2 protein (data not shown). In addition, the mAbs exhibited moderate (2D11-IgG, 1A7-IgG) to strong (2A2-IgG, 1A1-IgG) cross-reactivity to mouse ROR1 (Fc-mROR1). Overall, mAb 2A2 exhibited stronger reactivity to hROR1 and mROR1 than the other three mAbs, which was confirmed by surface plasmon resonance studies (see below and data not shown). This prompted us to focus on mAb 2A2 and clone, express and purify a mAb 2A2-based immunotoxin in dsFv format we named BT-1 (see Materials and Methods and Fig. 2S). Like the parent mAb 2A2, BT-1 showed specific binding to hROR1-ECD in ELISA (OD 405 value = 1.38) and did not bind hROR2-Fc (OD 405 value = 0, i.e., equal to background).

Cell surface binding of anti-hROR1 mAbs and BT-1. Both 2A2-IgG and 2D11-IgG exhibited dose-dependent (0.001–10 µg/mL) binding to MCL cell lines JeKo-1, Mino and *ex vivo* primary CLL and MCL cells, but not to normal B cells or EBV-transformed B-cell lines established from healthy donor PBMC (Fig. 2 and data not shown). By contrast, mAbs 1A1-IgG and 1A7-IgG, despite binding to purified proteins in ELISA, did not show any binding to ROR1-positive cells or cell lines (data not shown), and further studies are needed to understand this discrepancy. In agreement with our previous report using GaROR1 pAbs,⁹ the binding of 2A2-IgG revealed variations in the level of ROR1 expression (differences in MFI) among samples from individual CLL patients and similarly, among samples from individual MCL patients (Fig. 2A and B). However, ROR1 expression was uniform in all malignant B cells in each sample (Fig. S1). Subsequent studies showed that the binding was specific to the malignant cells (CD5⁺CD19⁺ cells) from CLL and MCL patients; other PBMC subpopulations in CLL and MCL patients or CD19-positive cells from healthy donors were not recognized (Fig. S1 and data not shown). Titration of 2A2-IgG showed significant binding at a concentration as low as 1 ng/mL (~6.5 pM), suggesting a high affinity/avidity interaction (data not shown). In addition, mAb 2A2-IgG bound to all MCL cell lines tested (HBL-2, JeKo-1, Mino and Rec-1), but not to Burkitt

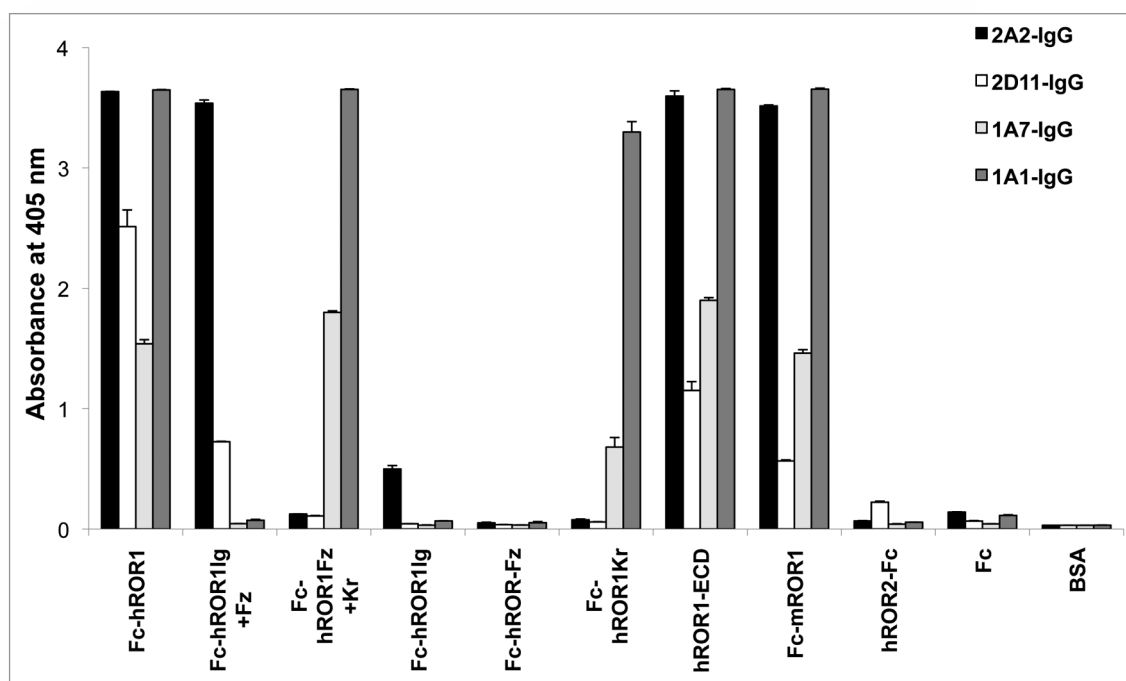


Figure 1. Specificity and epitope mapping of anti-hROR1 mAbs. ELISA plates were coated with 100 ng/50 μ L/well indicated recombinant fusion protein antigens. Different dilutions of mAbs 2A2-IgG (black bars), 2D11-IgG (open bars), 1A1-IgG (dark gray bars) or 1A7-IgG (light gray bars) were added (50 μ L/well) and data obtained with 1 μ g/mL alone is shown. The binding of the mAbs was detected using DaM-HRP as described in the Materials and Methods. Values represent arithmetic mean \pm standard deviation of triplicates for each condition, and similar results were obtained in three independent experiments. The data for BT-1, and positive control pAbs (GaROR1 and GaROR2) are provided in the text.

lymphoma cell lines (Raji, Ramos and Daudi), EBV-transformed B-cell lines (EBV-7475, RGC-EBV) or CLL cell lines (MEC-1, MEC-2 and 232-B4) (Fig. 2C and data not shown).

Similarly, like the parent mAb 2A2-IgG, immunotoxin BT-1 showed dose dependent binding to primary CLL and MCL cells and to the MCL cell lines JeKo-1 and Mino (Fig. 2A, B and D). The binding of BT-1 was restricted to the CD5⁺/19⁺ subpopulation in the PBMC samples from CLL and MCL patients (Fig. 2A and B). No significant binding above background was seen with B cells, T cells or other PBMC from healthy donors, and ROR1-negative B-cell lines RGC-EBV, Daudi, Raji and Ramos (Fig. 2D and data not shown).

Kinetic and thermodynamic analysis of 2A2-IgG and BT-1 binding to hROR1. To further investigate the affinity/avidity of 2A2-IgG and BT-1 in real time and label-free manner, we measured their interaction with hROR1 by surface plasmon resonance. First, hROR1-ECD or Fc-hROR1 (ligand) was immobilized on a CM5 sensor chip and mAb 2A2-IgG was run in the mobile phase (analyte). Regardless of the monovalent (hROR1-ECD) or bivalent (Fc-hROR1) nature of the ligand, 2A2-IgG showed a fast association (k_{on}) followed by a slow dissociation (k_{off}) resulting in observed equilibrium binding constants (K_D) of 0.12 nM and 0.42 nM, respectively (Table 1 and Fig. S3). Next, in a reverse orientation, 2A2-IgG was captured as ligand on a CM5 chip, and hROR1-ECD or Fc-hROR1 were run as analytes. Whereas the association rates of the two analytes to the mAb did not differ much in this setting, monovalent hROR1-ECD dissociated faster than bivalent Fc-hROR1, presumably due

to the lack of an avidity gain in the former. Consequently, monovalent binding showed a significant decrease in the observed K_D values (0.79 nM vs. 32.6 nM) with approximately 40-fold lower affinity (Table 1 and Fig. S3).

ROR1-immunotoxin BT-1 revealed a fast association rate similar to that seen with 2A2-IgG in binding Fc-hROR1. However, in comparison to bivalent 2A2-IgG, monovalent BT-1 exhibited a more than 100-fold faster dissociation rate, resulting in an observed K_D value of 64.9 nM (Table 1 and Fig. S3). Notably, the difference between the observed K_D values of analytes 2A2-IgG and BT-1 was similar to that found for analytes Fc-hROR1 and hROR1-ECD, revealing the strong avidity gain conferred by bivalency when the antibody or the antigen was in solution phase.

ROR1-mediated internalization. Internalization of cell surface bound anti-ROR1 mAb was measured as described before for pAbs.⁹ Both primary CLL cells and MCL cell lines exhibited partial internalization (approximately 30–45%) of cell surface bound 2A2-IgG (at 4°C) upon subsequent incubation at 37°C (Fig. 3A and B, and data not shown). Internalization was noticed as early as 30 min, reached a plateau by 2 h and no further increase was observed with prolonged incubation up to 6 h (data not shown). Internalization of cell surface bound mAbs was efficiently blocked in the presence of a chemical inhibitor, PAO, during incubation at 37°C (Fig. 3A and B). These results with mAbs are in agreement with our previous observation with GaROR1 pAbs using primary CLL cells.⁹ A similar level of internalization was observed when biotinylated 2A2-IgG was used, although

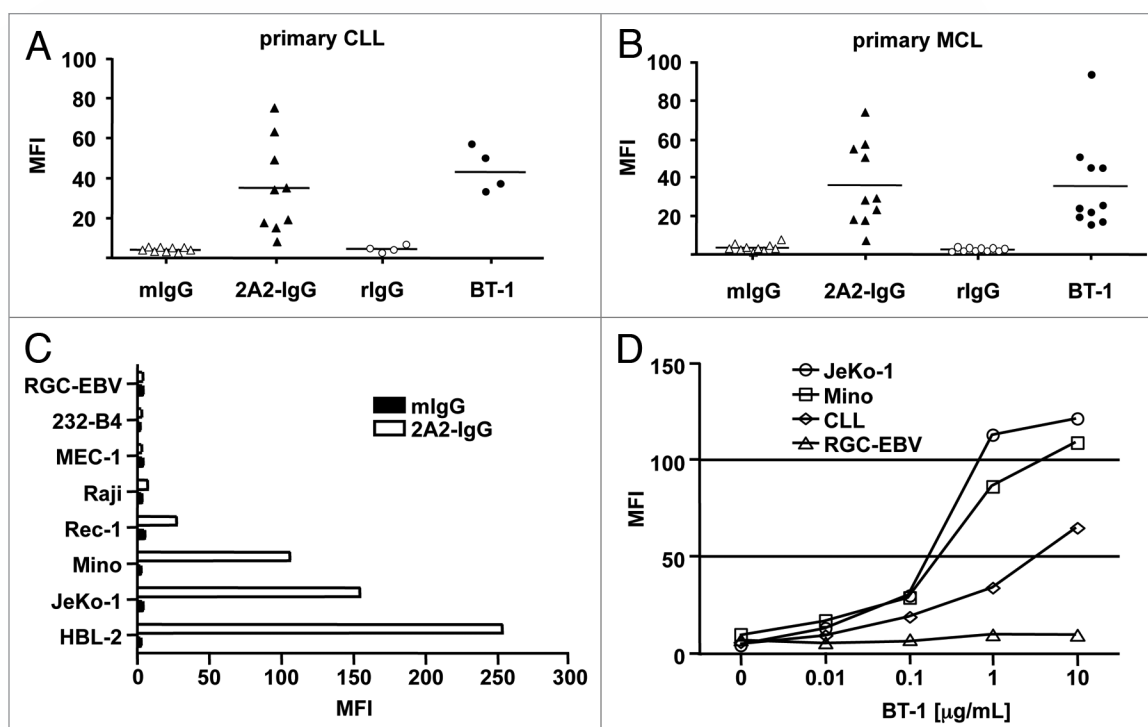


Figure 2. Cell surface binding of 2A2-IgG and BT-1. Primary CLL (A) primary MCL (B) cells and B cell lines (C) were incubated with 1 $\mu\text{g/mL}$ 2A2-IgG or BT-1 (D). In parallel controls, cells were incubated with 1 $\mu\text{g/mL}$ mouse IgG (mIgG) or rabbit IgG (rIgG). (D) Three B cell lines (JeKo-1, Mino and RGC-EBV) and primary CLL cells from a representative patient were incubated with different amounts of BT-1. Cell surface bound antibodies were detected using Dy-GaM (for mIgG and 2A2-IgG) or RaPEA followed by Dy-GaR (for BT-1). In (A and B), each data point represents an individual patient sample.

Table 1. Binding kinetics and thermodynamics of 2A2-IgG and BT-1

Ligand	Analyte	Binding	k_{on} [$10^5 \text{ s}^{-1} \text{ M}^{-1}$]	k_{off} [10^{-4} s^{-1}]	Observed K_{D} [10^{-9} M]
hROR1-ECD (direct)	2A2-IgG	Bivalent	15.2	1.8	0.12
Fc-hROR1 (direct)	2A2-IgG	Bivalent	8.1	3.4	0.42
2A2-IgG (captured)	Fc-hROR1	Bivalent	2.3	1.8	0.79
2A2-IgG (captured)	hROR1-ECD	Monovalent	2.4	77.7	32.6
Fc-hROR1 (direct)	BT-1	Monovalent	5.7	371.4	64.9

The indicated ligands were either directly immobilized on a CM5 chip (rows 1, 2 and 5) or captured with rabbit anti-mouse IgG-Fc pAbs as detailed in Materials and Methods. The association (k_{on}), dissociation (k_{off}) rate constants and the observed equilibrium dissociation constant (K_{D}) of the interactions were calculated using the Biacore X100 evaluation software.

the MFI was lower compared with non-biotinylated 2A2-IgG. To further rule out the possibility that bound mAb dissociated from the cell surface during incubation at 37°C, we used fluorochrome (Atto-488) conjugated 2A2-IgG (Atto-488-2A2-IgG). This allowed simultaneous visualization of internalized (direct fluorescence) and surface retained (indirect fluorescence) mAb in non-permeabilized cells. Direct measurement of Atto-488 signals in JeKo-1 cells remained the same before and after incubation at 37°C. This is because both the internalized and cell surface retained antibody molecules are detected simultaneously, suggesting there was no dissociation of bound mAb. By contrast, indirect measurement using a fluorochrome-conjugated secondary antibody (Dy-GaM) detects only Atto-488-2A2-IgG retained on the cell surface in non-permeabilized cells. As expected, there was a clear reduction in signal upon 37°C incubation (Fig. 3A),

indicating that internalization took place. Additional experiments with another MCL cell line (Mino), as well as primary CLL and MCL cells showed similar levels of internalization of 2A2-IgG (Fig. 3B and data not shown).

Internalization of cell surface bound immunotoxin is a key requirement for mediating cytotoxicity. Results showed that cell surface bound BT-1 disappeared in MCL cell lines, as well as in primary CLL and MCL cells, following incubation at 37°C (Fig. 3C and data not shown). However, given the weaker binding kinetics of BT-1 (Table 1), along with the observations that disappearance was greater (60–80%) than that of 2A2-IgG and not prevented by PAO (Fig. 3C), it is likely that dissociation contributed to this disappearance. Nonetheless, a small amount of internalized BT-1 could potentially deliver toxin into target cells and induce apoptosis.

Induction of apoptosis by BT-1. Three independent assays were performed to determine the ability of BT-1 to kill target cells. First, cell surface exposure of PS was detected by Annexin-V binding and was interpreted as a measure of apoptosis. ROR1-positive (JeKo-1) and ROR1-negative (Daudi and Raji) cell lines were incubated at 37°C in the absence or presence of different amounts of BT-1 (0.01–100 µg/mL) for 20, 46, 64 and 75 h. While BT-1 induced dose and time dependent killing (apoptosis) of JeKo-1 cells, Daudi and Raji cells were not killed (Fig. 4S). Similarly, another ROR1-positive cell line, HBL-2 exhibited 100% apoptosis when cultured with as little as 1 µg/mL (16 nM) BT-1 for three days, and the ROR1-negative cell line, RGC-EBV showed no increase from the background level of apoptosis when cultured with up to 100 µg/mL (1,600 nM) of BT-1 for three days (Fig. 4). As expected, the untargeted small molecule drug camptothecin was able to induce apoptosis in all cell lines regardless of ROR1 expression, indicating that ROR1-negative cell lines are not refractory to apoptosis (data not shown).

Second, change in the mitochondrial membrane potential was measured as an indicator of apoptosis. HBL-2 and RGC-EBV cell lines were cultured for 24 h in the absence or presence of 1 µg/mL BT-1 and subsequently incubated with 12.5 nM DiOC₂(3) and washed before flow cytometry. A drop in the red fluorescence intensity (as well as green fluorescence intensity, data not shown), which indicated a change in mitochondrial membrane potential ($\Delta\psi$), was noted in HBL-2 cells when cultured with BT-1, but not in RGC-EBV cells (Fig. 5A and C). Lower concentrations of BT-1 (0.01–0.1 µg/mL) induced a lower drop of fluorescence intensity in HBL-2 cells (data not shown). Addition of 50 µM carbonylcyanide-3-chlorophenylhydrazide (CCCP), a nonspecific mitochondrial membrane destabilizer, during incubation with DiOC₂(3) served as a positive control and it induced change in mitochondrial membrane potential in both cell lines regardless of the presence of BT-1 (data not shown).

Third, intracellular activated caspase-3 was detected as an early indicator of apoptosis. HBL-2 and RGC-EBV cells were cultured 24 h in the absence or presence of 1 µg/mL BT-1, and subsequently stained with a rabbit mAb against human activated caspase-3. Almost all HBL-2 cells cultured with BT-1 exhibited the presence of activated caspase-3, whereas RGC-EBV cells showed only background levels of staining except for a small population of cells (Fig. 5B and D). Collectively, these results demonstrated that BT-1 induced apoptosis in the ROR1-positive HBL-2 cell line.

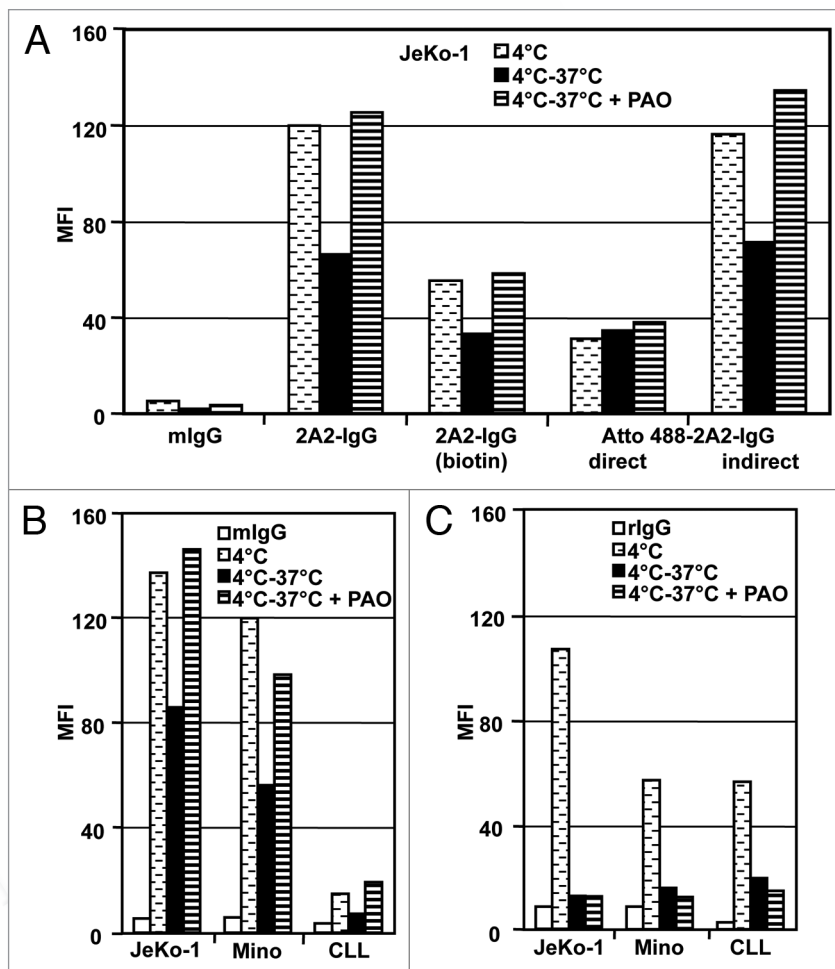


Figure 3. ROR1-mediated internalization of cell surface bound antibodies. (A) JeKo-1 cells were incubated for 1 h at 4°C with 1 µg/mL mlgG, 2A2-IgG, biotin-2A2-IgG or Atto 488-2A2-IgG. Cells in each group were washed and divided into three aliquots for further incubation at 4°C (partly hashed bars), or at 37°C in the absence (black bars) or presence (fully hashed bars) of 10 µM PAO. The antibody retained on the surface was detected with Dy-GaM (for mlgG and 2A2-IgG) or SA-PE (for biotin-2A2-IgG). The Atto 488-2A2-IgG binding was detected either by direct fluorescence or indirectly using Dy-GaM. As a control, Atto 488-mlgG was used, and gave a background staining of MFI = 3.7 (direct) and 6.1 (indirect). (B and C) MCL cell lines (JeKo-1 and Mino) and primary CLL cells (data from a representative patient is shown) were incubated at 4°C for 1 h with 1 µg/mL 2A2-IgG (B) or BT-1 (C). Open bars depict controls incubated with mlgG (B) or rIgG (C). Aliquots were made and subsequently incubated at 37°C as described above and the antibody retained on cell surface was detected with Dy-GaM (B) or Dy-GaR (C).

To further confirm BT-1 as a targeted drug, four MCL cell lines expressing different levels of ROR1 (HBL-2, JeKo-1, Mino and Rec-1) were cultured in the absence or presence of different amounts of BT-1 (0.001–100 µg/mL) for three days. Four ROR1-negative cell lines (RGC-EBV, Daudi, Raji and 232-B4) served as controls. Based on Annexin-V binding, all ROR1-positive cell lines showed a dose-dependent increase in apoptosis and none of the ROR1-negative cell lines showed significant apoptosis over background (Fig. 6). The sensitivity to BT-1-induced apoptosis appeared to be influenced by target antigen density (ROR1 expression levels) on the MCL cell lines (Table 2). The HBL-2 cells had the highest ROR1 expression (based on both MFI and

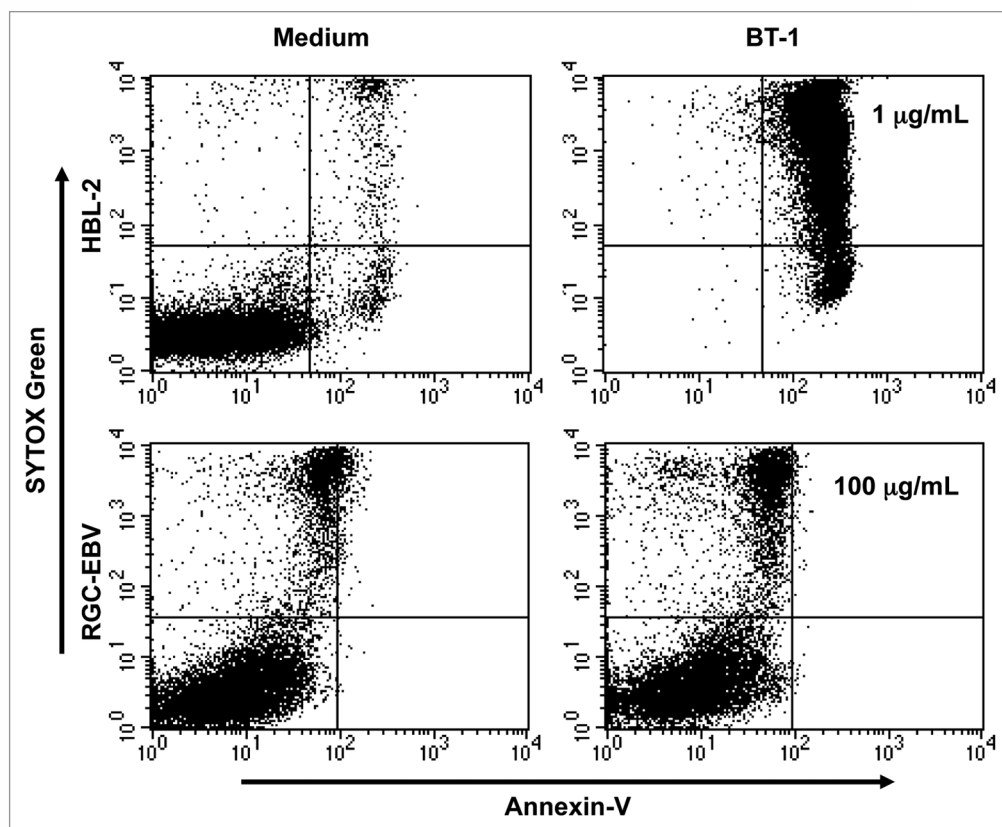


Figure 4. BT-1-induced apoptosis in ROR1-positive cells. A ROR1-positive (HBL-2) and a ROR1-negative (RGC-EBV) cell line were cultured in the absence (medium alone) or presence of BT-1 at 1 µg/mL and 100 µg/mL, respectively, for 3 d at 37°C. Apoptotic cells were detected with Annexin-V staining.

ABC values) and the EC_{50} of BT-1 was approximately 0.01 µg/mL (0.16 nM), followed by JeKo-1 at 0.1 µg/mL (1.6 nM) and Mino at 1.0 µg/mL (16 nM). The Rec-1 cells were highly sensitive to BT-1 EC_{50} 0.001 µg/mL (0.016 nM), but there was a discrepancy in the measurement of ROR1 expression. In repeated experiments, while the MFI values were low (Fig. 2C), the ABC values were high (Table 2) for Rec-1 cells and the reason for this inconsistency is not known. Next, as an independent correlate, the level of the anti-apoptotic protein, BCL2 was measured. The amount of intracellular BCL2 varied among the ROR1-positive MCL cell lines, and paralleled their sensitivity to BT-1 (Table 2). It is interesting to note that the highly sensitive Rec-1 cells have the lowest BCL2 level.

Discussion

Targeted therapy is a novel approach in the treatment and control of cancers, and has the potential to enhance the therapeutic efficacy, minimize undesirable side effects and help achieve a better clinical outcome in patients. With respect to B-cell malignancies, we and others have demonstrated uniform and restricted expression of ROR1 in CLL and MCL cells, and suggested its potential as a therapeutic target.^{9-11,36} The present study describes the development, characterization and validation of four mouse mAbs against hROR1. Subsequently, we focused on one of the two mAbs (2A2-IgG) that selectively bound ROR1-positive primary CLL

and MCL cells as well as MCL cell lines and revealed the overall strongest reactivity with hROR1 and mROR1. Nonetheless, 2A2-IgG alone or after conversion to chimeric mouse/human IgG1 (data not shown) and three chimeric rabbit/human IgG1 against ROR1³⁰ failed to induce significant direct cytotoxicity, CDC or ADCC in primary CLL cells or ROR1-positive MCL cell lines. Such unarmed mAb-mediated effector functions have generally been demonstrated in cells with high target antigen density (e.g., CDC activity of rituximab on human B cells with >40,000 CD20 molecules/cell).³⁷ Our previous study estimated the ROR1 density on CLL cells to be between 2,500 and 7,000 molecules/cell,⁹ which may be below the threshold needed for unarmed mAbs to mediate effector functions.^{38,39} It is also possible that the effector functions of unarmed mAbs against ROR1 are influenced by epitope location.⁴⁰

Knowing that cell surface ROR1 mediated internalization of bound antibody in primary CLL cells and MCL cell lines, the use of a ROR1-immunotoxin was sought to potentially overcome this limitation. The induction of profound apoptosis by mAb 2A2-derived ROR1-immunotoxin BT-1 in dsFv-PE38 format in ROR1-positive MCL cell lines, but not in ROR1-negative B-cell lines validated that ROR1 can function as a therapeutic target. The specific cytotoxicity induced by BT-1 was confirmed by three independent measurements: PS exposure to cell surface, change in mitochondrial membrane potential and activation of caspase-3, events that have been well documented in apoptotic

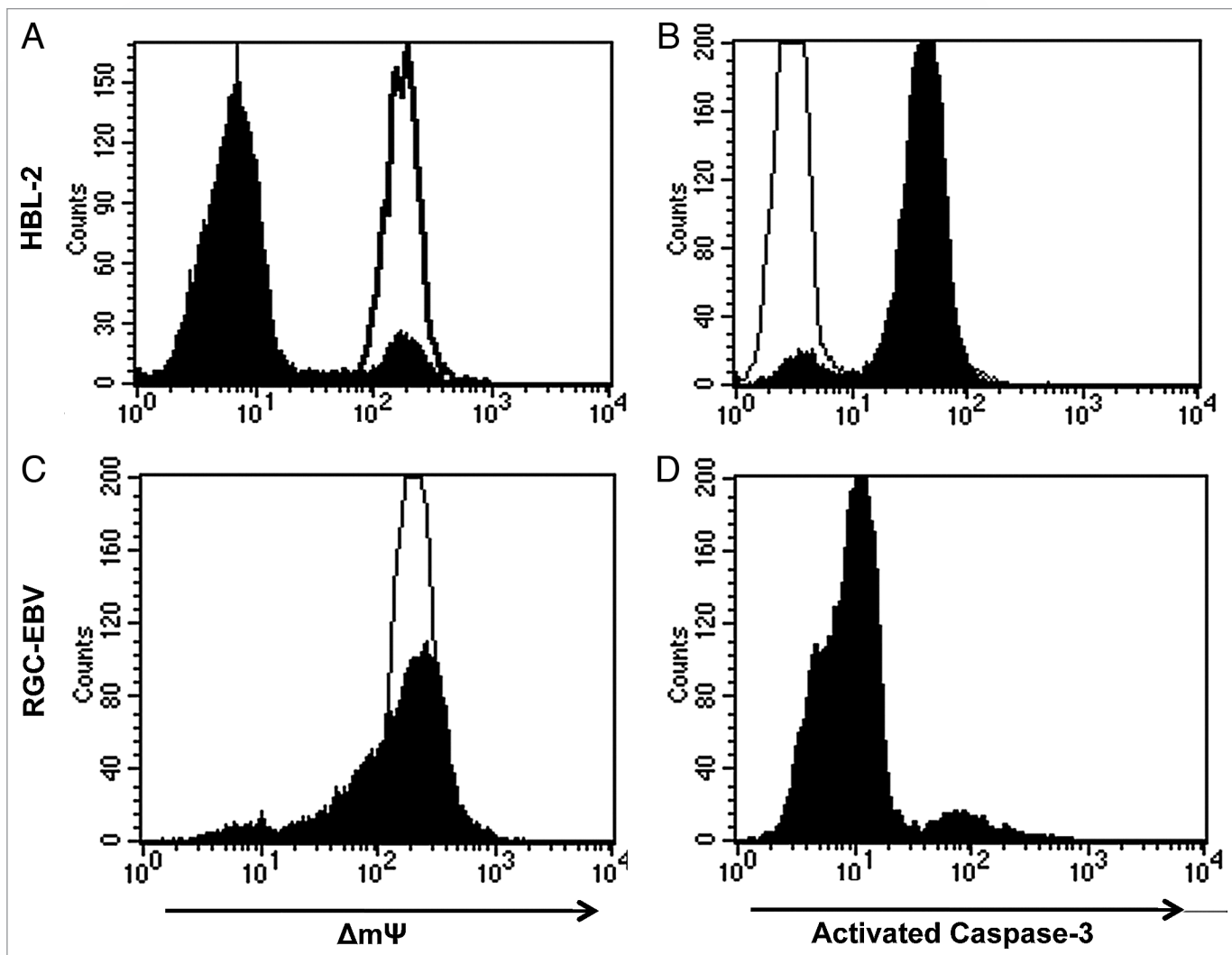


Figure 5. Early events of apoptosis induced by BT-1. HBL-2 (A and B) or RGC-EBV (C and D) cells were cultured in the absence (open histogram) or presence (filled histogram) of BT-1 at 1 μ g/mL for 24 h at 37°C. For measuring the mitochondrial membrane potential, $\Delta m\Psi$ (A and C), the cells were washed in warm medium and incubated with 12.5 nM DiOC₂(3) in DMSO or DMSO alone for 30 min at 37°C. Separate tubes were set up as positive control where 50 μ M CCCP in DMSO was added along with DiOC₂(3). All cells were washed once before flow cytometry. The x-axis represents DiOC₂(3) fluorescence intensity = $\Delta m\Psi$. For intracellular staining for activated caspase-3 (B and D), separate tubes were set up, and the cells were permeabilized, fixed and stained with PE-conjugated rabbit anti-human activated caspase-3 antibody. In (D), the open and filled histograms are superimposed. The data obtained in a representative experiment is shown.

cell death. The maximum effect was seen after approximately 3 d and this is in agreement with other studies using PE38-based immunotoxins.¹⁶ The dose-response curves depicted differences in BT-1 sensitivity among different MCL cell lines, and this could reflect cell specific intrinsic factors as regulators of apoptosis.

A number of parameters determine the efficacy of immunotoxins. First, the affinity of a mAb or a mAb fragment (e.g., dsFv) to its target antigen largely determines the stability of the antibody/antigen complex on the cell surface. A head-to-head comparison of the observed K_D values of bivalent 2A2-IgG (0.42 nM) and 2A2-derived monovalent BT-1 (64.9 nM) binding to immobilized Fc-ROR1 revealed an approximately 150-fold difference in BT-1 binding. Assuming that similar binding might occur with cell surface ROR1 and given that the half-life of the antigen/antibody interaction equals $\ln 2/k_{off}$ the

estimated cell surface retention of BT-1 would be 19 sec compared with 34 min for 2A2-IgG. Although the dose-response curves with BT-1 showed robust killing of ROR1-positive MCL lines at low concentration (with EC_{50} values of 16 pM to 16 nM), there is likely room for improvement. Other PE38-based immunotoxins that target different antigens on malignant B cells (CD19 and CD22) or mesothelioma (mesothelin) showed higher potency presumably due to higher affinity, i.e., lower dissociation rate constants, for the respective antigens, resulting in longer cell surface retention.⁴¹ Currently, we are looking into different antibody engineering strategies to improve the affinity or avidity of BT-1. Alternatively, a new panel of chimeric rabbit/human mAbs to ROR1 that was selected by phage display in the monovalent Fab format for high affinity binding to ROR1 and reveals dissociation rate constants up to 120-fold

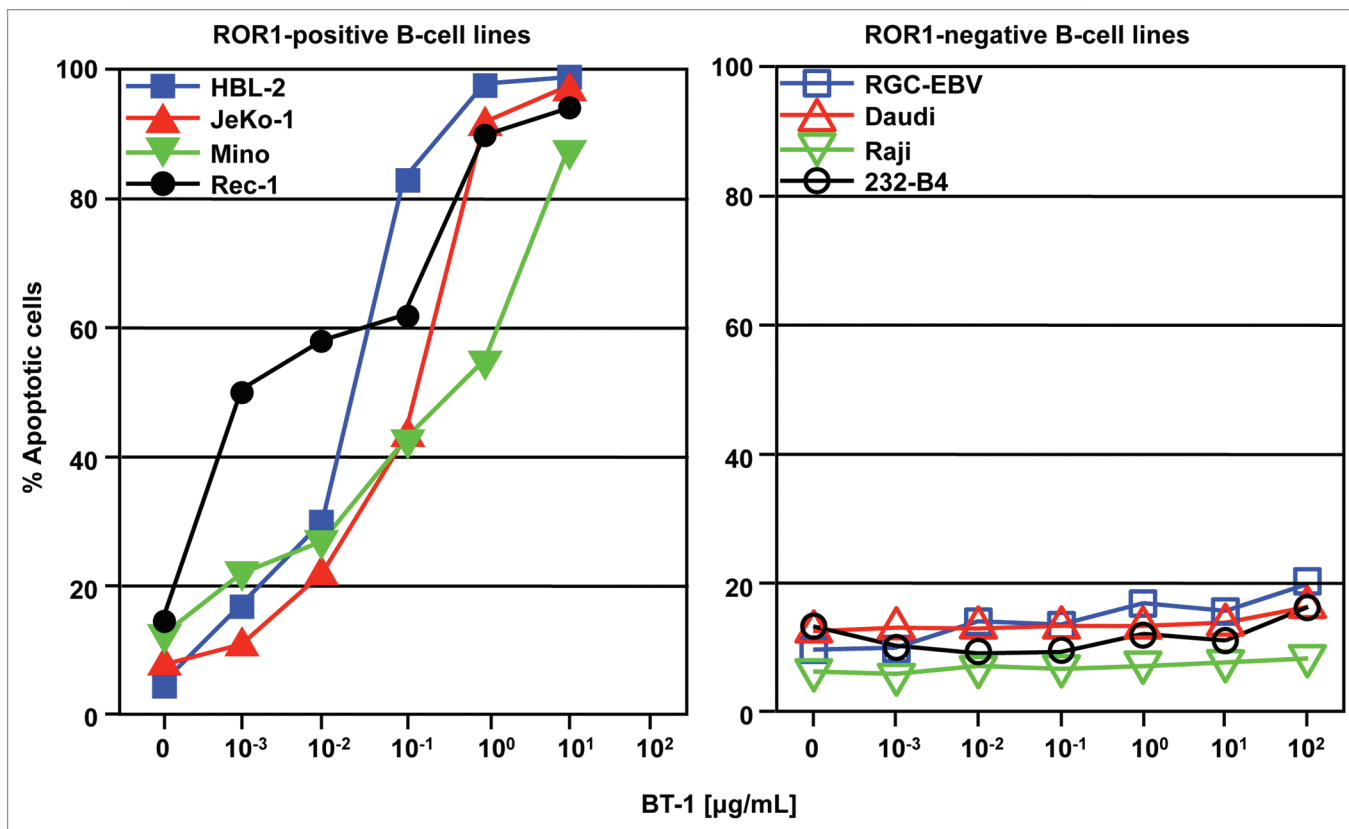


Figure 6. Immunotoxin induced dose-dependent apoptosis in MCL cell lines. Four ROR1-positive MCL cell lines (filled symbols; HBL-2, blue square; JeKo-1, red triangle; Mino, green triangle; Rec-1, black circle) and four ROR1-negative B cell lines (open symbols; RGC-EBV, blue square; Daudi, red triangle; Raji, green triangle; 232-B4, black circle) were cultured in the absence or presence of different amounts of BT-1 (1 ng/mL–100 µg/mL) for 3 d at 37°C. The percentage of apoptotic cells was determined by Annexin-V staining. The data presented is representative of three independent experiments.

Table 2. ROR1 expression levels and BT-1 sensitivity

Target cells	BCL2 ^a (MFI)	ROR1 ^b (ABC)	BT-1 sensitivity EC ₅₀ [nM] ^c
HBL-2	78	25440	0.16
JeKo-1	29	12484	1.6
Mino	41	10144	16
Rec-1	18	27386	0.016

^aIntracellular BCL2 expression was determined using a PE-conjugated mouse anti-human BCL2 mAb; PE-conjugated isotype control was used for background staining. ^bROR1 density was determined by measuring ABC of 2A2-IgG-AlexaFluor-647; polyclonal mIgG-AlexaFluor-647 was used as control. ^cConcentration of BT-1 required to induce apoptosis in 50% of the cells. Similar values were obtained in three independent experiments.

lower than BT-1,³⁰ could be employed for the next generation of ROR1-immunotoxins.

Second, the target antigen density on the cell surface could influence immunotoxin efficacy. Our data showed an approximately 1000-fold difference in EC₅₀ values among ROR1-positive MCL cell lines (0.016 nM for Rec-1, 0.16 nM for HBL-2, 1.6 nM for JeKo-1 and 16 nM for Mino) and overall this

paralleled ROR1 expression levels among these cell lines. A correlation between target antigen density and apoptosis induction was also reported for CD22- and FCRL1-immunotoxins.^{16,42} However, preliminary results indicate that Rec-1 cells expressed the lowest level of the anti-apoptotic protein BCL2 compared with the other MCL cell lines we tested. It is conceivable that BCL2 levels in addition to the level of other anti-apoptotic proteins (e.g., MCL1, survivin, XIAP) can influence the efficacy of BT-1 as has been reported for other immunotoxins.^{43,44}

Third, our epitope mapping studies indicated that 2A2-IgG (the parent antibody of BT-1) bound to the membrane distal Ig-domain of ROR1. Immunotoxins generated from antibodies recognizing different epitopes on the same antigen showed significant differences in their potency in vitro.^{45,46} An immunotoxin binding to a membrane proximal epitope on the target antigen, CD2, induced higher cytotoxicity than those binding to distal epitopes.⁴⁷ Therefore, it may be worthwhile to generate ROR1-immunotoxins based on mAbs recognizing different epitopes and compare their abilities to kill ROR1-expressing cells.

Fourth, the rate of internalization of surface bound immunotoxin could affect its efficacy. A recent study compared the efficacy of two immunotoxins, RFB4 (Fv)-PE38 also known as BL22 (anti-CD22) and FMC63 (Fv)-PE38 (anti-CD19) on

lymphoma cell lines. Despite lower cell surface expression of CD22, rapid internalization of large amounts of BL22 made CD22 a better target than CD19 present in high density.⁴⁸ There was clear evidence for BT-1-mediated apoptosis in ROR1-positive cell lines within 24 h, but how much BT-1 was actually internalized is unknown. Further studies on the membrane dynamics of ROR1, intracellular trafficking of BT-1 and its degradation rate are required to better understand and improve the efficacy of next generation ROR1-immunotoxins.

Despite the profound cytotoxicity induced by BT-1 in vitro, the surface plasmon resonance data indicated relatively fast dissociation of the monovalent BT-1 compared with its parent antibody, and it is likely that this could be a limitation in exploring its in vivo activity. We are currently working on generating different formats of ROR1 immunotoxins with a goal to enhance the affinity/avidity, and minimize potential immunogenicity. The efficacy of improved immunotoxins can be tested in vivo using MCL cell lines as xenografts in nude mice. The cytotoxicity studies described here were based on MCL cell lines and, unlike primary CLL and MCL cells, they do not undergo spontaneous apoptosis in vitro. A more clinically relevant system for evaluating the ability of ROR1-immunotoxins to kill primary CLL and MCL cells may be a recently developed mouse model with adoptively transferred human primary CLL cells that retain ROR1 expression in vivo.⁴⁹

In summary, as a proof of concept, we have demonstrated that a ROR1-immunotoxin can induce apoptosis resulting in robust killing of ROR1-expressing MCL cell lines in vitro. Owing to its exquisite specificity, BT-1 could function as a leukemia/lymphoma specific therapeutic agent in vivo, and unlike unarmed mAbs, would not depend on the effector machinery such as complement proteins, NK cells, macrophages or T cells as these may not be optimally available in cancer patients. BT-1 provides a platform for next generation ROR1-immunotoxins with defined modifications in both antibody and toxin portion designed to enhance affinity and efficacy, as well as minimize immunogenicity.^{50,51} In addition, combination strategies with small molecule inhibitors of anti-apoptotic proteins could help to mitigate the opposing effects and boost the efficacy of BT-1 and next generation ROR1-immunotoxins.

Materials and Methods

Patient samples and cell lines. Patients with CLL and MCL were enrolled in institutional review board-approved studies at the National Institutes of Health (NIH), Bethesda, MD and blood samples were obtained with written informed consent. Blood samples from healthy donors were obtained from the Department of Transfusion Medicine, Clinical Center, NIH. Peripheral blood mononuclear cells (PBMC) were prepared by density gradient separation of whole blood on lymphocyte separation medium (MP Biochemicals, 50494) and cryopreserved until use. The CLL cell lines MEC-1 and MEC-2 were obtained from DSMZ and 232-B4 was a gift from Dr. Anders Rosén (Linköping University). The MCL cell lines used in this study (JeKo-1, HBL-2, Mino and Rec-1) have been characterized,²⁸

and Burkitt lymphoma cell lines (Raji, Ramos and Daudi) were obtained from ATCC. EBV-transformed lymphoblastoid cell lines were generated from PBMC from a healthy donor (EBV-7475) and a patient with CLL (RGC-EBV) by following standard procedure;²⁹ both of these were oligoclonal suggesting their origin from normal B cells (unpublished observation). All cell lines were maintained in vitro in RPMI-1640 supplemented with 2 mM Glutamax, 10% (v/v) (GIBCO, 61870) fetal bovine serum (FBS) (GIBCO, 10437), 20 mM HEPES (GIBCO, 15630080), 100 IU/mL penicillin, 100 µg/mL streptomycin sulfate (GIBCO #15140-148), 50 µM β-mercaptoethanol (Sigma, M-7522) and 1 mM sodium pyruvate (GIBCO, 11360070).

Mouse mAbs against human ROR1. A panel of recombinant ROR1 proteins were cloned, expressed and purified as described in reference 30; Fc-hROR1, hROR1-ECD, Fc-hROR1Ig+Fz (Ig+Fz), Fc-hROR1Fz+Kr (Fz+Kr), Fc-hROR1Ig (Ig), Fc-hROR1Fz (Fz), Fc-hROR1Kr (Kr), human Fc (Fc) and Fc-mROR1. Purified human ROR2-Fc was purchased from R&D Systems (custom order).

Mouse anti-hROR1 mAbs were custom generated (Precision Antibody). In brief, mice were immunized with Fc-hROR1, and after three booster injections with hROR1-ECD serum antibody response against ROR1 was detected. Hybridomas were generated using the immune spleen cells. Screening of about 100 hybridoma clones yielded four clones 2A2, 2D11, 1A1 and 1A7 that secreted mAbs that bound specifically to ROR1. The four hybridoma clones were grown in BD Cell mAb medium (Animal Component Free, Becton Dickinson, 220513) using CELLline Flasks (Becton Dickinson, 353137) and supernatants were collected. HiTrap Protein G columns (GE Healthcare, 17-0404-01) were used to purify immunoglobulins (Ig) from the supernatants. Reduced SDS-PAGE analysis revealed only Ig heavy and light chain bands of expected molecular sizes for each mAb. The isotype of all four mAbs was determined to be mouse IgG1kappa using the Mouse Immunoglobulin Isotyping ELISA Kit (BD Pharmingen, 550487).

Preparation of ROR1-immunotoxin. Partial amino acid sequences from both variable domains of 2A2-IgG were obtained by custom LC-MS/MS analysis on tryptic digests of SDS-PAGE resolved heavy and light chain polypeptides (Alphalyse, custom order). Based on this information, the mouse V gene families were identified using Ig BLAST (www.ncbi.nlm.nih.gov/igblast). Oligonucleotides aligning to the signal peptide encoding DNA sequences of the V_K and V_H gene families and to the C_K and C_{γ1}1 constant domain encoding DNA sequences were used to amplify 2A2-V_L and 2A2-V_H by RT-PCR from total RNA isolated from 2A2 hybridoma cells. DNA sequencing of the PCR products yielded the complete amino acid sequences of the 2A2-V_H and 2A2-V_L polypeptides (*International Patent Application PCT/US2010/032208*). The 2A2-based immunotoxin BT-1 was generated following the procedure described in reference 31 with some changes detailed below. Optimized for expression in *Escherichia coli* (*E. coli*), the DNA sequences encoding 2A2-V_H and 2A2-V_L polypeptides were custom synthesized with the following modifications (DNA 2.0); 2A2-V_H included a *Nde*I site at the 5' end and a *Hind*III site at the 3'

end; 2A2- V_L included a *NdeI* site at the 5' end and an *EcoRI* site at the 3' end. In addition, the codons for residues 45 in 2A2- V_H and 99 in 2A2- V_L , both present in framework regions, were substituted with a codon for cysteine to allow pairing of V_H and V_L polypeptides and yield disulphide linked Fv (dsFv) after refolding. These DNA sequences were cloned into separate stocks of pJ201 plasmids. *NdeI/HindIII*-digested 2A2- V_H was cloned into a T7 expression vector (pRB98) creating an in-frame fusion with a DNA sequence encoding truncated *Pseudomonas* exotoxin A (PE38). Separately, *NdeI/EcoRI*-digested 2A2- V_L was cloned into pRB98 (thereby removing the PE38 encoding DNA sequence).³¹ The two expression plasmids were separately electroporated into *E. coli* strain BL21 (λ DE3) cells (ElectroMax; Invitrogen, 11319-019) and 1 L culture of bacteria transformed with each plasmid was grown with IPTG induction. The bacterial pellets were processed and inclusion body proteins were pooled and allowed to refold. The refolded ROR1-immunotoxin, 2A2(dsFv)-PE38 (named BT-1), was purified by two sequential ion exchange chromatography steps using Q-Sepharose column (GE Healthcare, 17-5159-01) and Mono-Q column (GE Healthcare, 17-5166-01) followed by a gel filtration chromatography step using a HiLoad 16/60 Superdex S200 prep grade column (GE Healthcare, 17-1069-01), all in conjunction with an ÄKTA-FPLC system using Unicorn software (Amersham Pharmacia Biotech). The purity of BT-1 was validated by a single sharp peak seen in the gel filtration chromatography profile, its retention time was in close proximity with that of bovine serum albumin (BSA, Sigma-Aldrich, A-7906) in the same column, and SDS-PAGE analysis revealed a single band of the expected size (Fig. S2). Purified BT-1 was stored in PBS pH 7.2 at -70°C until use.

Enzyme-linked immunosorbent assay (ELISA). To determine the specific reactivity and epitope mapping of anti-ROR1 mAbs, 96-well plates (Clear Microplate; R&D Systems, DY990) were coated with indicated recombinant ROR1 proteins (100 ng in 50 μ L/well) in PBS pH 7.2 overnight at 4°C. The next day, the wells were washed with 10 mM Tris-buffered saline with 0.1% (v/v) Triton X-100 pH 7.2 (TBST) using an automatic plate washer (Beckman Coulter), and blocked with 300 μ L/well 3% (w/v) BSA in PBS pH 7.2 for 2 h at 25°C. After one wash cycle, 50 μ L of primary anti-ROR1 antibodies (mouse mAbs 2A2-IgG, 2D11-IgG, 1A1-IgG, 1A7-IgG, goat polyclonal antibodies (pAbs) against ROR1 (R&D Systems, AF2000), goat pAbs against ROR2 (R&D Systems, AF2064) or BT-1) diluted in 1% (w/v) BSA in PBS pH 7.2 were added in different concentrations and incubated at 25°C for 2 h. For BT-1 alone, the wells were washed again, 50 μ L/well polyclonal rabbit anti-pseudomonas exotoxin A serum (RaPEA, Sigma-Aldrich, P2318) was added at 1:300 final dilution and incubated for 2 h. After two wash cycles, 50 μ L/well corresponding detection antibodies were added (horseradish peroxidase conjugated donkey anti-mouse IgG, DaM-HRP (Jackson ImmunoResearch Laboratories, 715-036-150); donkey anti-goat IgG, DaG-HRP (705-035-147) or donkey anti-rabbit IgG, DaR-HRP (711-036-152) at 1:1,000 dilution in 1% (w/v) BSA in PBS pH 7.2 and incubated for 1 h at 25°C. After two wash cycles, the enzymatic activity of

bound antibody was determined by adding the HRP substrate ABTS (Roche Applied Science, 10102946001) and measuring the absorbance at 405 nm (and 490 nm to allow auto correction) in a VersaMax microplate reader (Molecular Devices).

Surface plasmon resonance. The binding kinetics of anti-hROR1 antibody formats (2A2-IgG and BT-1) and hROR1 were studied by measuring the surface plasmon resonance using a Biacore X-100 instrument and Biacore reagents and software (GE Healthcare). This was done either by direct coupling or capture of the ligands at comparable and low densities to minimize the mass transfer effect. For direct coupling, a CM5 sensor chip (GE Healthcare, BR-1000-12) was activated with 1-ethyl-3-(3-dimethylaminopropyl) carbodiimide hydrochloride and N-hydroxysuccinimide for subsequent ligand immobilization. The fusion proteins Fc-hROR1 and hROR1-ECD in 10 mM sodium acetate pH 5.0 were immobilized in flow cell 1 (FC-1) at a density of 160–300 resonance units (RU) in separate sensor chips. The FC-2 in each chip served as control (without ligand) to allow instant background correction. The chips were deactivated with 1 M ethanolamine hydrochloride, pH 8.5. The analytes, 2A2-IgG and BT-1, were diluted in 1x HBS-EP⁺ running buffer pH 7.4 (10 mM HEPES, 150 mM NaCl, 3 mM EDTA and 0.05% (v/v) Surfactant P20), and five different concentrations of analytes (range 2.5–100 nM) were run in duplicates at a flow rate of 30 μ L/min. The chips were regenerated using glycine-HCl pH 2.0 without significant loss of binding capacity. In the capture method, first polyclonal rabbit anti-mouse IgG was immobilized on a CM5 chip to give an approximate final density of 9,790 RU in both FC-1 and FC-2 (Mouse Antibody Capture Kit; GE Healthcare, BR-1008-38) and deactivated following the manufacturer's recommended procedure. Subsequently, the ligand (2A2-IgG) was captured at 1 μ g/mL (predetermined concentration) to give an approximate density of 200 RU in FC-1, with FC-2 serving as control. The analytes (hROR1-ECD and Fc-hROR1) were run at five different concentrations (range 3–1,000 nM) in duplicates as described above. Calculation of association (k_{on}) and dissociation (k_{off}) rate constants was based on a 1:1 Langmuir binding model for both monovalent and bivalent interactions. The equilibrium dissociation constant (K_D) was calculated from k_{off}/k_{on} .

Flow cytometry. Approximately 5×10^5 cells were incubated with different concentrations of affinity-purified 2A2-IgG or normal polyclonal mouse IgG (mIgG; Jackson ImmunoResearch Laboratories, 015-000-003) for 45 min at 4°C. After two washes with FACS buffer (2% (v/v) FBS in PBS pH 7.2), the cells were incubated for 45 min at 4°C with DyLight-649 conjugated, affinity pure F(ab)₂ preparation of goat anti-mouse IgG (Dy-GaM; Jackson ImmunoResearch Laboratories, 115-496-146) or APC-conjugated goat anti-mouse IgG, Fc fragment specific (APC-GaM, 115-136-071) at 1:500 final dilution. For primary CLL and MCL cells, the malignant B cells were gated using CD5/CD19 Simultest reagent (BD Biosciences, 340396). Similarly, for staining with ROR1-immunotoxin BT-1, target cells were incubated with various concentrations of BT-1, followed by normal polyclonal rabbit IgG (rIgG, Jackson ImmunoResearch Laboratories, 011-000-002) or the secondary antibody (RaPEA)

at 1:300 final dilution and then with DyLight-649-conjugated, affinity pure F(ab)₂ preparation of goat anti-rabbit IgG (Dy-GaR; Jackson ImmunoResearch Laboratories, 111-496-144) at 1:500 final dilution. Cells were washed twice with FACS buffer in each step and, after two final washes, they were resuspended in FACS buffer and 5 µg/mL propidium iodide (P.I., Sigma-Aldrich, P4170) was added to exclude dead cells from analysis. For the detection of intracellular BCL2, the cells were washed in PBS, then with BD Perm/Wash buffer (BD Biosciences, 554723), and subsequently fixed and permeabilized for 20 min using BD Cytotfix/Cytoperm buffer (BD Biosciences, 554722) and washed again with BD Perm/Wash buffer. The cells were stained with PE-conjugated mouse anti-human BCL2 mAb or an isotype control (BD Biosciences, BCL2 set #556535). A total of 20,000 gated events were collected for each sample using FACSCalibur instrument (BD Biosciences) and data were analyzed using CellQuest software. The values were depicted as mean fluorescence intensity (MFI).

ROR1-mediated internalization of mAbs. ROR1-mediated internalization was determined by measuring the decrease in surface bound (at 4°C) anti-ROR1 mAb after incubation at 37°C.⁹ Approximately 2×10^6 target cells were incubated with 1 µg/mL unconjugated 2A2-IgG for 1 h on ice (4°C) in RPMI-5% (v/v) FBS. The cells were washed twice with ten volumes of medium and resuspended as 5×10^5 aliquots in medium. One aliquot was left on ice and the others were incubated at 37°C for various periods of time either without or with 10 µM phenylarsine oxide (PAO; Sigma-Aldrich, P3075). Next, the cells were washed with medium and all samples were incubated with Dy-GaM at 1:500 final dilution. After 1 h incubation on ice, the cells were washed and resuspended in FACS buffer (see above) with 5 µg/mL P.I. and analyzed by flow cytometry. Additional experiments were performed using biotinylated 2A2-IgG prepared with the BiotinTag Microbiotinylation kit (Sigma-Aldrich, BIOTAG), and detected by streptavidin-conjugated phycoerythrin (SA-PE, BD Biosciences, 554061). Furthermore, directly labeled 2A2-IgG was used to simultaneously measure cell surface bound and internalized antibody. For this, mIgG (as control) and 2A2-IgG were coupled to Atto-488 following the manufacturer's recommended procedure (Novus Biologicals, 733-0010). While Atto488 fluorescence collectively measured cell surface bound and internalized 2A2-IgG, only the cell surface bound fraction was detectable with a secondary antibody (Dy-GaM) in non-permeabilized cells. Internalization of BT-1 was analyzed by sequential incubations with RaPEA and Dy-GaR (Jackson ImmunoResearch Laboratories, 111-496-144) as described above.

Determination of ROR1 density. The number of ROR1 molecules on the target cell surface was determined using the Quantum Simply Cellular Microbeads Kit (Bangs Laboratories, 815B) as described before in reference 9, with following modifications. First, 2A2-IgG was directly labeled using Alexa Fluor 647 Protein Labeling Kit (Molecular Probes, A20173) following the recommended procedure to obtain 2A2-IgG-AF647 conjugate. In parallel, polyclonal mouse IgG (mIgG) was used to obtain mIgG-AF647. Approximately, 1×10^6 cells were

incubated for 30 min at 4°C in the dark with predetermined saturating concentration of 2A2-IgG-AF647. As control, mIgG-AF647 was used. In parallel, the quantum beads were incubated with predetermined saturating concentration of 2A2-IgG-AF647 conjugate. The cells and the beads were washed three times, resuspended in the FACS buffer and the MFI were determined by flow cytometry with the same instrument settings. Using the QuickCal software (Bangs Laboratories), a calibration curve was generated by plotting MFI vs. the antigen binding capacity (ABC) of the beads. The delta MFI values of each sample (2A2-IgG-AF647 minus mIgG-AF647) was used to determine the ABC of the sample and considered to represent the antigen (ROR1) density on the cell surface.

Immunotoxin-mediated cytotoxicity. ROR1-immunotoxin (BT-1) induced death of target cells was detected by three independent methods: (a) detection of cell surface exposure of phosphatidylserine (PS),³² (b) measurement of changes in mitochondrial membrane potential³³ and (c) intracellular detection of activated caspase-3.^{34,35} ROR1-expressing and non-expressing cell lines (2.5×10^5 cells) were incubated at 37°C for various periods of time in RPMI-5% (v/v) FBS in the absence or presence of different amounts of BT-1 (0.01–100 µg/mL). For PS exposure, both BT-1 treated and untreated cells were washed in Annexin-V binding buffer (ABB), incubated with Alexa Fluor 647-conjugated Annexin-V (Invitrogen, A23204) and SYTOX Green (Invitrogen, S7020) following the manufacturer's recommended procedure and subjected to flow cytometry. Camptothecin (Sigma-Aldrich, C9911) was used (10 µM) as a positive control to induce apoptosis. The percentage of apoptotic cells was determined as follows: % Apoptosis = % Annexin-V-positive cells + % Annexin-V-positive and SYTOX Green-positive cells/total cells analyzed \times 100. The SYTOX Green-positive and Annexin-V-negative cells were considered necrotic cells, and the double negative cells were considered live cells. The change in mitochondrial membrane potential ($\Delta m\Psi$) has been considered to be one of the early events in apoptosis, and such a change leads to accumulation of cationic cyanine dyes in cells that can be measured by flow cytometry. Untreated and BT-1 treated cells were incubated with a predetermined concentration (12.5 nM) of 3,3'-diethyloxycarbocyanine iodide (DiOC₂(3); MitoProbe kit, Molecular Probes, M34150) following the manufacturer's recommended procedure. The cells were washed once and red and green fluorescence intensities were measured. Red fluorescence intensity increases due to dye stacking in cells with active mitochondria and decreases in cells with disrupted mitochondria. Both qualitative and quantitative changes in fluorescence intensity of the dye were measured and depicted as histogram. The caspase family of cysteine proteases plays a key role in apoptosis. In particular, caspase-3 is activated during early stages of apoptosis, and the active enzyme cleaves survival proteins such as BCL2 and PARP, resulting in apoptosis. To determine intracellular levels of activated caspase-3, BT-1 treated and untreated cells were washed in PBS, fixed and permeabilized using BD Cytotfix/Cytoperm for 20 min at 25°C, washed with BD Perm/Wash buffer. Cells were then stained

with PE-conjugated rabbit anti-active caspase-3 antibody (BD Biosciences, 550821) and subjected to flow cytometry.

Disclosure of Potential Conflicts of Interest

The authors declare no competing financial interest.

Acknowledgments

This work was funded by the Intramural Research Program of the National Institutes of Health [National Cancer Institute and National Heart, Lung and Blood Institute]. We thank Mr. Michael G. Kennedy and Dr. Jiahui Yang for the generation of recombinant ROR1 proteins, Dr. Anders Rosen for providing

the 232-B4 cell line and Dr. William G. Telford and Ms. Veena Kapoor for maintaining the flow cytometry core facility.

Authors' Contributions

S.B. and C.R. designed the research; S.B. performed all the experiments and wrote the manuscript; A.W. and W.H.W. provided access to patient samples; C.R., A.W., W.H.W. and I.P. critically reviewed the manuscript.

Supplemental Material

Supplemental material can be found at: www.landesbioscience.com/journals/mabs/article/19870

References

- Masiakowski P, Carroll RD. A novel family of cell surface receptors with tyrosine kinase-like domain. *J Biol Chem* 1992; 267:26181-90; PMID:1334494.
- Rosenwald A, Alizadeh AA, Widhopf G, Simon R, Davis RE, Yu X, et al. Relation of gene expression phenotype to immunoglobulin mutation genotype in B cell chronic lymphocytic leukemia. *J Exp Med* 2001; 194:1639-47; PMID:11733578; <http://dx.doi.org/10.1084/jem.194.11.1639>.
- Klein U, Tu Y, Stolovitzky GA, Mattioli M, Cattoretti G, Husson H, et al. Gene expression profiling of B cell chronic lymphocytic leukemia reveals a homogeneous phenotype related to memory B cells. *J Exp Med* 2001; 194:1625-38; PMID:11733577; <http://dx.doi.org/10.1084/jem.194.11.1625>.
- Barna G, Mihalik R, Timár B, Tömböl J, Csenge Z, Sebestyén A, et al. ROR1 expression is not a unique marker of CLL. *Hematol Oncol* 2011; 29:17-21; PMID:20597086; <http://dx.doi.org/10.1002/hon.948>.
- Gentile A, Lazzari L, Benvenuti S, Trusolino L, Comoglio PM. Ror1 is a pseudokinase that is crucial for Met-driven tumorigenesis. *Cancer Res* 2011; 71:3132-41; PMID:21487037; <http://dx.doi.org/10.1158/0008-5472.CAN-10-2662>.
- MacKeigan JP, Murphy LO, Blenis J. Sensitized RNAi screen of human kinases and phosphatases identifies new regulators of apoptosis and chemoresistance. *Nat Cell Biol* 2005; 7:591-600; PMID:15864305; <http://dx.doi.org/10.1038/ncb1258>.
- Choudhury A, Derkow K, Daneshmanesh AH, Mikaelsson E, Kiaii S, Kokhaei P, et al. Silencing of ROR1 and FMOD with siRNA results in apoptosis of CLL cells. *Br J Haematol* 2010; 151:327-35; PMID:20813009; <http://dx.doi.org/10.1111/j.1365-2141.2010.08362.x>.
- Li P, Harris D, Liu Z, Liu J, Keating M, Estrov Z. Stat3 activates the receptor tyrosine kinase like orphan receptor-1 gene in chronic lymphocytic leukemia cells. *PLoS One* 2010; 5:11859; PMID:20686606; <http://dx.doi.org/10.1371/journal.pone.0011859>.
- Baskar S, Kwong KY, Hofer T, Levy JM, Kennedy MG, Lee E, et al. Unique cell surface expression of receptor tyrosine kinase ROR1 in human B-cell chronic lymphocytic leukemia. *Clin Cancer Res* 2008; 14:396-404; PMID:18223214; <http://dx.doi.org/10.1158/1078-0432.CCR-07-1823>.
- Fukuda T, Chen L, Endo T, Tang L, Lu D, Castro JE, et al. Antisera induced by infusions of autologous Ad-CD154-leukemia B cells identify ROR1 as an oncofetal antigen and receptor for Wnt5a. *Proc Natl Acad Sci USA* 2008; 105:3047-52; PMID:18287027; <http://dx.doi.org/10.1073/pnas.0712148105>.
- Daneshmanesh AH, Mikaelsson E, Jeddí-Tehrani M, Bayat AA, Ghods R, Ostadkarampour M, et al. Ror1, a cell surface receptor tyrosine kinase is expressed in chronic lymphocytic leukemia and may serve as a putative target for therapy. *Int J Cancer* 2008; 123:1190-5; PMID:18546292; <http://dx.doi.org/10.1002/ijc.23587>.
- Lapalombella R, Andritsos L, Liu Q, May SE, Browning R, Pham LV, et al. Lenalidomide treatment promotes CD154 expression on CLL cells and enhances production of antibodies by normal B cells through a PI3-kinase-dependent pathway. *Blood* 2010; 115:2619-29; PMID:19965642; <http://dx.doi.org/10.1182/blood-2009-09-242438>.
- Pastan I. Immunotoxins containing Pseudomonas exotoxin A: a short history. *Cancer Immunol Immunother* 2003; 52:338-41; PMID:12700949.
- Pastan I, Hassan R, Fitzgerald DJ, Kreitman RJ. Immunotoxin therapy of cancer. *Nat Rev Cancer* 2006; 6:559-65; PMID:16794638; <http://dx.doi.org/10.1038/nrc1891>.
- Kreitman RJ, Chaudhary VK, Kozak RW, FitzGerald DJ, Waldman TA, Pastan I. Recombinant toxins containing the variable domains of the anti-Tac monoclonal antibody to the interleukin-2 receptor kill malignant cells from patients with chronic lymphocytic leukemia. *Blood* 1992; 80:2344-52; PMID:1421405.
- Decker T, Oelsner M, Kreitman RJ, Salvatore G, Wang QC, Pastan I, et al. Induction of caspase-dependent programmed cell death in B-cell chronic lymphocytic leukemia by anti-CD22 immunotoxins. *Blood* 2004; 103:2718-26; PMID:14525789; <http://dx.doi.org/10.1182/blood-2003-04-1317>.
- FitzGerald DJ, Willingham MC, Pastan I. Pseudomonas exotoxin—immunotoxins. *Cancer Treat Res* 1988; 37:161-73; PMID:2908624; http://dx.doi.org/10.1007/978-1-4613-1083-9_11.
- Nagata S, Onda M, Numata Y, Santora K, Beers R, Kreitman RJ, et al. Novel anti-CD30 recombinant immunotoxins containing disulfide-stabilized Fv fragments. *Clin Cancer Res* 2002; 8:2345-55; PMID:12114439.
- Hassan R, Cohen SJ, Phillips M, Pastan I, Sharon E, Kelly RJ, et al. Phase I clinical trial of the chimeric anti-mesothelin monoclonal antibody MORAb-009 in patients with mesothelin-expressing cancers. *Clin Cancer Res* 2010; 16:6132-8; PMID:21037025; <http://dx.doi.org/10.1158/1078-0432.CCR-10-2275>.
- Kreitman RJ, Pastan I. Immunotoxins in the treatment of hematologic malignancies. *Curr Drug Targets* 2006; 7:1301-11; PMID:17073592; <http://dx.doi.org/10.2174/138945006778559139>.
- Sarnovsky R, Tendler T, Makowski M, Kiley M, Antignani A, Traini R, et al. Initial characterization of an immunotoxin constructed from domains II and III of cholera exotoxin. *Cancer Immunol Immunother* 2010; 59:737-46; PMID:20091030; <http://dx.doi.org/10.1007/s00262-009-0794-4>.
- Reiter Y, Brinkmann U, Lee B, Pastan I. Engineering antibody Fv fragments for cancer detection and therapy: disulfide-stabilized Fv fragments. *Nat Biotechnol* 1996; 14:1239-45; PMID:9631086; <http://dx.doi.org/10.1038/nbt1096-239>.
- Hwang J, Fitzgerald DJ, Adhya S, Pastan I. Functional domains of Pseudomonas exotoxin identified by deletion analysis of the gene expressed in *E. coli*. *Cell* 1987; 48:129-36; PMID:3098436; [http://dx.doi.org/10.1016/0092-8674\(87\)90363-1](http://dx.doi.org/10.1016/0092-8674(87)90363-1).
- Kreitman RJ, Squires DR, Stetler-Stevenson M, Noel P, FitzGerald DJ, Wilson WH, et al. Phase I trial of recombinant immunotoxin RFB4(dsFv)-PE38 (BL22) in patients with B-cell malignancies. *J Clin Oncol* 2005; 23:6719-29; PMID:16061911; <http://dx.doi.org/10.1200/JCO.2005.11.437>.
- Kreitman RJ, Stetler-Stevenson M, Margulies I, Noel P, FitzGerald DJ, Wilson WH, et al. Phase II trial of recombinant immunotoxin RFB4(dsFv)-PE38 (BL22) in patients with hairy cell leukemia. *J Clin Oncol* 2009; 27:2983-90; PMID:19414673; <http://dx.doi.org/10.1200/JCO.2008.20.2630>.
- Kreitman RJ, Margulies I, Stetler-Stevenson M, Wang QC, FitzGerald DJ, Pastan I. Cytotoxic activity of disulfide-stabilized recombinant immunotoxin RFB4(dsFv)-PE38 (BL22) toward fresh malignant cells from patients with B-cell leukemias. *Clin Cancer Res* 2000; 6:1476-87; PMID:10778980.
- Kreitman RJ, Chaudhary VK, Waldman T, Willingham MC, FitzGerald DJ, Pastan I. The recombinant immunotoxin anti-Tac(Fv)-Pseudomonas exotoxin 40 is cytotoxic toward peripheral blood malignant cells from patients with adult T-cell leukemia. *Proc Natl Acad Sci USA* 1990; 87:8291-5; PMID:2236041; <http://dx.doi.org/10.1073/pnas.87.21.8291>.
- Weniger MA, Rizzatti EG, Pérez-Galán P, Liu D, Wang Q, Munson PJ, et al. Treatment-induced oxidative stress and cellular antioxidant capacity determine response to bortezomib in mantle cell lymphoma. *Clin Cancer Res* 2011; 17:5101-12; PMID:21712452; <http://dx.doi.org/10.1158/1078-0432.CCR-10-3367>.
- Aman P, Ehlin-Henriksson B, Klein G. Epstein-Barr virus susceptibility of normal human B lymphocyte populations. *J Exp Med* 1984; 159:208-20; PMID:6319530; <http://dx.doi.org/10.1084/jem.159.1.208>.
- Yang J, Baskar S, Kwong KY, Kennedy MG, Wiestner A, Rader C. Therapeutic potential and challenges of targeting receptor tyrosine kinase ROR1 with monoclonal antibodies in B-cell malignancies. *PLoS One* 2011; 6:21018; PMID:21698301; <http://dx.doi.org/10.1371/journal.pone.0021018>.
- Pastan I, Beers R, Bera TK. Recombinant immunotoxins in the treatment of cancer. *Methods Mol Biol* 2004; 248:503-18; PMID:14970517.
- Andree HA, Reutelingersperger CP, Hauptmann R, Hemker HC, Hermens WT, Willems GM. Binding of vascular anticoagulant alpha (VACalpha) to planar phospholipid bilayers. *J Biol Chem* 1990; 265:4923-8; PMID:2138622.
- Cossarizza A, Salvioli S. Flow cytometric analysis of mitochondrial membrane potential using JC-1. *Curr Protoc Cytom* 2001; 9:14.
- Dai C, Krantz SB. Interferon gamma induces upregulation and activation of caspases 1, 3 and 8 to produce apoptosis in human erythroid progenitor cells. *Blood* 1999; 93:3309-16; PMID:10233883.
- Thornberry NA, Lazebnik Y. Caspases: enemies within. *Science* 1998; 281:1312-6; PMID:9721091; <http://dx.doi.org/10.1126/science.281.5381.1312>.

36. Hudecek M, Schmitt TM, Baskar S, Lupo-Stanghellini MT, Nishida T, Yamamoto TN, et al. The B-cell tumor-associated antigen ROR1 can be targeted with T cells modified to express a ROR1-specific chimeric antigen receptor. *Blood* 2010; 116:4532-41; PMID:20702778; <http://dx.doi.org/10.1182/blood-2010-05-283309>.
37. van Meerten T, van Rijn RS, Hol S, Hagenbeek A, Ebeling SB. Complement-induced cell death by rituximab depends on CD20 expression level and acts complementary to antibody-dependent cellular cytotoxicity. *Clin Cancer Res* 2006; 12:4027-35; PMID:16818702; <http://dx.doi.org/10.1158/1078-0432.CCR-06-0066>.
38. Mankaï A, Bordron A, Renaudineau Y, Martins-Carvalho C, Takahashi S, Ghedira I, et al. Purinergic box-1-mediated reduced expression of CD20 alters rituximab-induced lysis of chronic lymphocytic leukemia B cells. *Cancer Res* 2008; 68:7512-9; PMID:18794139; <http://dx.doi.org/10.1158/0008-5472.CAN-07-6446>.
39. Weitzman J, Betancur M, Boissel L, Rabinowitz AP, Klein A, Klingemann H. Variable contribution of monoclonal antibodies to ADCC in patients with chronic lymphocytic leukemia. *Leuk Lymphoma* 2009; 50:1361-8; PMID:19562616; <http://dx.doi.org/10.1080/10428190903026500>.
40. Daneshmanesh AH, Hojjat-Farsangi M, Khan AS, Jeddi-Tehrani M, Akhondi MM, Bayat AA, et al. Monoclonal antibodies against ROR1 induce apoptosis of chronic lymphocytic leukemia (CLL) cells. *Leukemia* 2012; PMID:22289919; <http://dx.doi.org/10.1038/leu.2011.362>.
41. Alderson RF, Kreitman RJ, Chen T, Yeung P, Herbst R, Fox JA, et al. CAT-8015: a second-generation pseudomonas exotoxin A-based immunotherapy targeting CD22-expressing hematologic malignancies. *Clin Cancer Res* 2009; 15:832-9; PMID:19188153; <http://dx.doi.org/10.1158/1078-0432.CCR-08-1456>.
42. Du X, Nagata S, Ise T, Stetler-Stevenson M, Pastan I. FCRL1 on chronic lymphocytic leukemia, hairy cell leukemia and B-cell non-Hodgkin lymphoma as a target of immunotoxins. *Blood* 2008; 111:338-43; PMID:17895404; <http://dx.doi.org/10.1182/blood-2007-07-102350>.
43. Bogner C, Dechow T, Ringshausen I, Wagner M, Oelsner M, Lutzny G, et al. Immunotoxin BL22 induces apoptosis in mantle cell lymphoma (MCL) cells dependent on Bcl-2 expression. *Br J Haematol* 2010; 148:99-109; PMID:19821820; <http://dx.doi.org/10.1111/j.1365-2141.2009.07939.x>.
44. Traini R, Ben-Josef G, Pastrana DV, Moskatel E, Sharma AK, Antignani A, et al. ABT-737 overcomes resistance to immunotoxin-mediated apoptosis and enhances the delivery of pseudomonas exotoxin-based proteins to the cell cytosol. *Mol Cancer Ther* 2010; 9:2007-15; PMID:20587662; <http://dx.doi.org/10.1158/1535-7163.MCT-10-0257>.
45. Godal A, Kumle B, Pihl A, Juell S, Fodstad O. Immunotoxins directed against the high-molecular-weight melanoma-associated antigen. Identification of potent antibody-toxin combinations. *Int J Cancer* 1992; 52:631-5; PMID:1399146; <http://dx.doi.org/10.1002/ijc.2910520423>.
46. Yazdi PT, Wenning LA, Murphy RM. Influence of cellular trafficking on protein synthesis inhibition of immunotoxins directed against the transferrin receptor. *Cancer Res* 1995; 55:3763-71; PMID:7641191.
47. Press OW, Martin PJ, Thorpe PE, Vitetta ES. Ricin A-chain containing immunotoxins directed against different epitopes on the CD2 molecule differ in their ability to kill normal and malignant T cells. *J Immunol* 1988; 141:4410-7; PMID:2461993.
48. Du X, Beers R, Fitzgerald DJ, Pastan I. Differential cellular internalization of anti-CD19 and -CD22 immunotoxins results in different cytotoxic activity. *Cancer Res* 2008; 68:6300-5; PMID:18676854; <http://dx.doi.org/10.1158/0008-5472.CAN-08-0461>.
49. Bagnara D, Kaufman MS, Calissano C, Marsilio S, Patten PE, Simone R, et al. A novel adoptive transfer model of chronic lymphocytic leukemia suggests a key role for T lymphocytes in the disease. *Blood* 2011; 117:5463-72; PMID:21385850; <http://dx.doi.org/10.1182/blood-2010-12-324210>.
50. Hansen JK, Weldon JE, Xiang L, Beers R, Onda M, Pastan I. A recombinant immunotoxin targeting CD22 with low immunogenicity, low nonspecific toxicity and high antitumor activity in mice. *J Immunother* 2010; 33:297-304; PMID:20445350; <http://dx.doi.org/10.1097/CJI.0b013e3181cd1164>.
51. Onda M, Beers R, Xiang L, Lee B, Weldon JE, Kreitman RJ, et al. Recombinant immunotoxin against B-cell malignancies with no immunogenicity in mice by removal of B-cell epitopes. *Proc Natl Acad Sci USA* 2011; 108:5742-7; PMID:21436054; <http://dx.doi.org/10.1073/pnas.1102746108>.